Available online at www.sciencedirect.com
SCIENCE DIRECT
Solid State Communications 137 (2006) 474–477
solid state communications
www.elsevier.com/locate/ssc

Electron transport in high quality undoped ZnO film grown by plasma-assisted molecular beam epitaxy

Yeon Sik Jung [a], Oleg V. Kononenko [a,b], Won-Kook Choi [a,*]

[a] Korea Institute of Science and Technology, Thin Film Materials Research Center, Cheongryang, P.O. Box 131, Seoul 130-650, South Korea
[b] Institute of Microelectronics Technology and High Purity Materials, Russian Academy of Science, 142432 Chernogolovka, Moscow Region, Russian Federation

Received 21 June 2005; received in revised form 29 November 2005; accepted 28 December 2005 by B. Jusserand
Available online 24 January 2006

Abstract

High quality ZnO films were grown on *c*-plane sapphire substrate using low temperature ZnO buffer layer by plasma-assisted molecular beam epitaxy. The film deposited at 720 °C showed the lowest value of full-width at half maximum for the symmetric (0002) diffraction peak of about 86 arcsec. The highest electron mobility in the films was about 103–105 cm^2/V s. From temperature-dependent Hall effect measurements, the mobility strongly depends on the dislocation density at low temperature region and the polar optical phonon scattering at high temperature, respectively. Moreover, by obtaining the activation energy of the shallow donors, it was supposed that hydrogen was source of n-type conductivity in as-grown ZnO films.

PACS: 73.50.−h; 73.61.Ga; 81.15.Hi

Keywords: A. Zinc oxide; B. Molecular beam epitaxy; C. Dislocation; E. Hall measurement

1. Introduction

ZnO, a II–VI semiconductor, has been extensively investigated because it has quite large exciton binding energy (E_{ex} = 60 meV) and high optical gain (g = 300 cm^{-1}) [1] at room temperature superior to other II–VI (ZnSe, 22 meV) and III–V (GaN, 25 meV) semiconductors. Even though several significant achievements in successful p-doping of ZnO [2–4] were reported, the lack of well-established reproducible p-type ZnO doping process still remains a provision for the realization of ZnO-based light emitting diode/laser diode. There have been many challenges to figure out the origins of an intrinsic shallow donor and a green emission [5–9]. Additionally, an electron transport in ZnO should also be well understood to fabricate highly efficient ZnO-based optoelectronic devices. For better understanding of electron mobility, electrical properties of ZnO single crystal with electron concentration of $n_e = 6\times10^{16}$ cm^{-3} and mobility μ = 205 cm^2/V s grown by seeded-vapor phase (SVP) was studied through temperature-dependent Hall effect (TDH) measurement [7–9]. Recently, it has been also reported that the insertion of a thin low temperature (LT) ZnO or MgO buffer layer or ZnO/MgO double buffer layer between ZnO film and substrate dramatically reduced the screw and edge dislocation, and thus an electron mobility of ZnO films was increased up to 137 cm^2/V s [10–13].

To date, there are few reports on the electron transport of ZnO thin films through TDH measurement. In the present work, high quality ZnO films were grown on sapphire substrate using LT ZnO buffer layer by plasma-assisted molecular beam epitaxy. The crystalline and optical properties are examined by X-ray ω-rocking curve (XRC) and Raman spectroscopy. Carrier concentration and Hall mobility were measured by the van der Pauw method. Through TDH in the temperature range of 10–300 K a dominant scattering mechanism which mainly contributes to electron transport is carefully studied and discussed.

2. Experiment

High quality ZnO thin films were grown on *c*-Al_2O_3 (1000) single crystal by plasma assisted molecular beam epitaxy. Metal Zn grains (6 N purity) were used and chemically active oxygen atoms were assisted by rf discharge at 450 W. Low temperature (LT) homo-buffer ZnO layer of 15 nm was deposited at 500 °C prior to the growth of thick ZnO at high temperature and then annealed in O plasma environment at 680–800 °C for 4 h. By the observation of RHEED pattern, layer by layer growth mode, 2D, was well maintained up to

* Corresponding author. Fax: +82 2 958 6851.
E-mail address: wkchoi@kist.re.kr (W.-K. Choi).

0038-1098/$ - see front matter © 2006 Elsevier Ltd. All rights reserved.
doi:10.1016/j.ssc.2005.12.038

760 °C, but it changed into Stranski–Krasnov mode, 3D, at 800 °C. The thickness of all the films was fixed at about 800 nm within the error of ±10% which was measured by optical interference method. Other growth conditions, including the growth of LT ZnO buffer layer, were well described in detail elsewhere [14,15]. The crystallinity was analyzed by X-ray diffraction and by obtaining ω-rocking curve over ZnO(0002) diffraction using X-ray diffractometer (Bruker AXS, D8 Discover). Atomic concentration was identified by time-of-flight secondary ion mass spectrometry (SIMS) using 7.9 keV Cs^+ ion for sputtering. TDH measurement was carried out by the van der Pauw at various temperature and then the mobility and concentration were also calculated.

3. Results and discussion

Table 1 summarizes the variations of full-width at half maximum (FWHM) of XRC for symmetric (0002) diffraction, Hall mobility and carrier concentration of the ZnO films grown at different substrate temperatures. At the temperature of 720–760 °C, quite high Hall mobility $\mu = 103$–$105\ cm^2/V\ s$ could be attained and corresponding electron concentrations are 2.2–$2.5 \times 10^{17}\ cm^{-3}$. The small value of FWHM of XRC for the symmetric (0002) diffraction peak, which reflects the tilt component of the in-plane mosaic misorientation (Tilt), indicates the low density of screw dislocations in the film. The film deposited at 720 °C showed the smallest value of FWHM of about 86 arcsec and it slightly increases to 92 arcsec for the film grown at 760 °C, though the mobility increases slightly up to 105 $cm^2/V\ s$. The result indicates that the increase of density of screw dislocation does not directly decrease the mobility, and which is coincident with the reported result [13].

Fig. 1 shows data of carrier concentration as a function of inverse temperature for the ZN-1 and ZN-2, obtained from TDH measurements. It can be seen that there is a large change in the slope of the curves at 60 and 120 K for ZN-1 and ZN-2 films, respectively. This sudden increase in the carrier concentration probably caused by impurity-band or defect-band effects [8].

Fig. 2 shows natural logarithm of Hall concentration as a function of inverse temperature. As you can see in Fig. 1, n increased after 60 K for ZN-1 grown at $T = 680$ °C and also increased after relatively higher temperature of 120 K for the sample grown at $T = 720$ K. Even though we could obtain n at low temperature region, n increases at low temperature ranges results from the mixed band and hopping mechanism [7] and

Table 1
Variations of Hall mobility and electron concentration for the ZnO thin films deposited at various temperature and the FWHM's taken from the ω-rocking curves for ZnO (0002) diffraction

T_s (°C)	FWHM of XRD ω-rocking curves ZnO (0002) (arcsec)	Hall mobility ($cm^2/V\ s$)	Carrier concentration (cm^{-3})
680 (ZN-1)	207	54.1	6.8×10^{17}
720 (ZN-2)	86	103.8	2.5×10^{17}
760 (ZN-3)	92	105.1	2.2×10^{17}
800 (ZN-4)	171	–	–

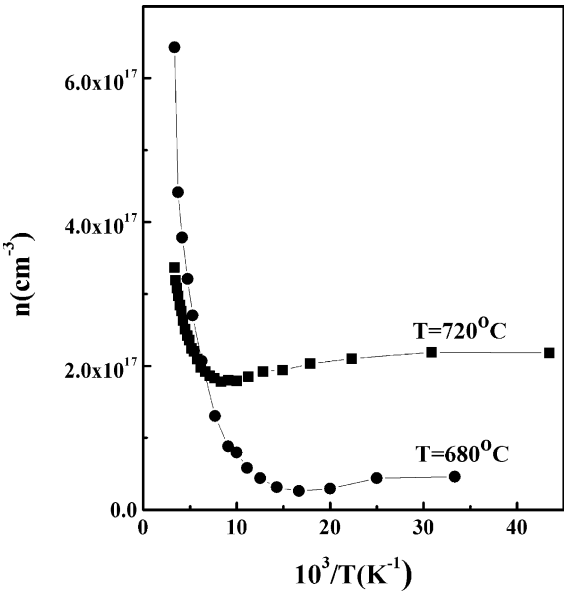

Fig. 1. Carrier concentration as a function of inverse temperature for the ZnO films grown at 680 °C (●, ZN-1) and 720 °C (■, ZN-2).

thus we disregard the data below 60 and 120 K in the fitting of statistical model involving only transport in the conduction band. Both data can be explicitly split into two groups and thus fitted into two different slopes of the lines. The slopes give us the activation energies of $E_{D1} = 36 \pm 2$ meV and $E_{D2} = 58 \pm 1.5$ meV for ZN-1 in the temperature range 110–60 and 300–110 K, respectively and $E_{D1} = 21 \pm 1.4$ meV and $E_{D2} = 43 \pm 1.5$ meV for ZN-2 in the temperature range 140–220 and 220–300 K, respectively. Look et al. in Ref. [9] reported that, a shallow donor with an activation energy 37 meV was found in the ZnO crystal and suggested that it can be correlated with Zn_i produced by electron-irradiation [8]. Using a first-principles calculations, Van de Walle showed that a most appropriate

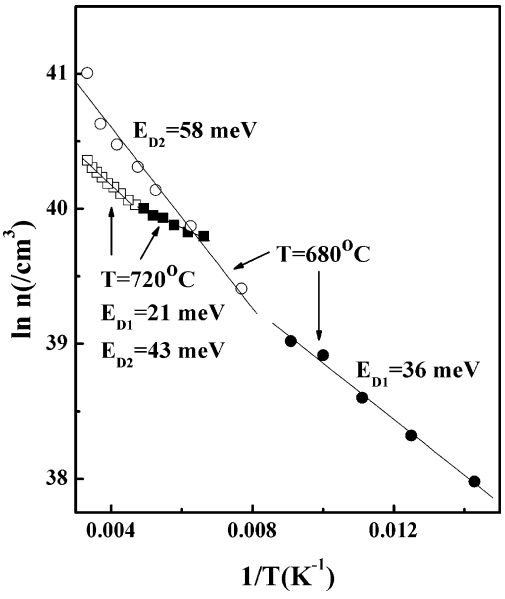

Fig. 2. Logarithmic Hall concentration as a function of inverse temperature for the ZnO films grown at 680 °C (●, ZN-1) and 720 °C (■, ZN-2).

candidate for a shallow donor was H [16,17] Hofmann et al. [18] experimentally measured that a donor at 35 ± 5 meV in ZnO was H. Experiments with H plasma exposed to ZnO also showed that a relative intensity of the donor-bound exciton at line I_4 increased with H-plasma exposure and decreased with annealing [19,20]. Recently Meyer et al. [21] found that a shallow donor with $E_D=46.1$ meV controls the conductivity and was attributed this particular donor to H by correlation with magnetic resonance experiment. The obtained values of $E_{D1}=36$ meV for ZN-1 and $E_{D2}=43$ meV for ZN-2 in Fig. 2 are very close to this value and this certainly denotes that this shallow donor is connected with H. Thus, we can attribute that hydrogen is the source of n-type conductivity in as-grown ZnO films. On the other hand, we need more experiments to clarify the nature of the lower energy donor (E_{D1} of ZN-2). Probably, this donor can be correlated with complexes of hydrogen with structural defects such as dislocations. The expected hydrogenic donor energy, for a static dielectric constant of 8.12 and an effective mass of $0.318m_0$, is 65 meV, which has been known to result from the V_0 and this value is comparable with $E_{D2}=58\pm1.5$ meV of ZN-2.

Fig. 3 shows the Hall mobility data as a function of temperature. The solid line is the fit to the mobility data, which is carried out using Rode's method of solving the Boltzmann transport equation [22]. The mobility data can be analyzed by taking five scattering mechanisms into account. The each component of the carrier mobility can be expressed using the following equations.

1. Ionized impurity scattering (μ_1):

$$\mu_1=\frac{128\sqrt{2\pi}k_0^2k_\infty^2}{e^3\sqrt{m_0}}\frac{\sqrt{(kT)^3}}{N_i\sqrt{\frac{m^*}{m_0}}\left[\ln(1+b)-\frac{b}{1+b}\right]}, \tag{1}$$

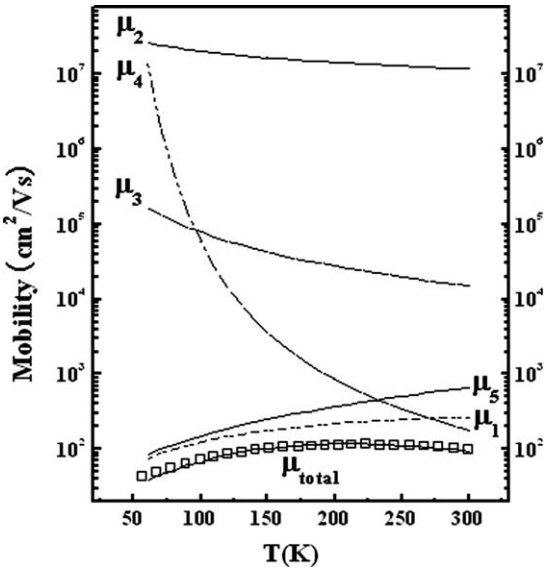

Fig. 3. Experimental (■) and calculated (solid line) Hall mobility as a function of temperature in ZnO thin films deposited at 720 °C (ZN-2) by plasma-assisted MBE. Different components of the mobility are also shown.

where

$$b=\frac{24m_0k_0k_\infty}{e^2\hbar^2}\frac{m^*(kT)^2}{m_0n'}, \tag{2}$$

where n' means free electron concentration.

2. Deformation potential scattering (μ_2):

$$\mu_2=\frac{\sqrt{8\pi}}{3}\frac{e\hbar^4C_l}{E_1^2\sqrt{(m^*)^5(kT)^3}}, \tag{3}$$

where C_l is the longitudinal elastic constant and E_1 is the deformation potential.

3. Piezoelectric scattering (μ_3):

$$\mu_3=\frac{16\sqrt{2\pi}}{3}\frac{\hbar^2}{e\sqrt{m^{*3}}}\frac{k_0k_\infty}{K^2\sqrt{kT}}, \tag{4}$$

where K is the piezoelectric coefficient.

4. Polar optical phonon scattering (μ_4):

$$\mu_4=0.199\sqrt{\frac{T}{300}}\left(\frac{e}{e_c^*}\right)^2\sqrt{\left(\frac{m_0}{m^*}\right)^3}(10^{22}M)(10^{23}V_a)\times(10^{-13}\omega_{lo})(e^z-1)G(z), \tag{5}$$

$$z=\frac{\hbar\omega_{lo}}{kT}, \tag{6}$$

where e_c^* is the Callen effective charge, M is the reduced mass, V_a is the volume of the unit cell, and ω_{lo} is the angular frequency of longitudinal optical phonons.

5. Dislocation scattering (μ_5):

$$\mu_5=\frac{30\sqrt{2\pi}k_0k_\infty d^2\sqrt{(kT)^3}}{e^3f^2m^{*2}\lambda_dN_{dis}}, \tag{7}$$

$$\lambda_d=\sqrt{\frac{k_0k_\infty kT}{e^2n}}, \tag{8}$$

where d is the distance between acceptor centers along the dislocation line, f is the occupation probability of the acceptor centers, λ_d is the Debye length, and N_{dis} is the dislocation density. Using Matthiessen's rule, the total carrier mobility can be obtained as follows:

$$\frac{1}{\mu_{total}}=\frac{1}{\mu_1}+\frac{1}{\mu_2}+\frac{1}{\mu_3}+\frac{1}{\mu_4}+\frac{1}{\mu_5}. \tag{9}$$

The contribution of different scattering components to total carrier mobility depends on parameters such as relative low-frequency dielectric constant k_0, relative high-frequency dielectric constant k_∞, longitudinal elastic constant C_l, deformation potential E_1, Debye temperature T_D, polaron effective mass m^*, piezoelectric coefficient K, dislocation density N_{dis}, distance between acceptor centers or dangling bonds d, and compensation ratio (ratio of acceptor concentration to donor one) N_A/N_D. Except for N_{dis} and

N_A/N_D, the values for these parameters were taken from Ref. [22] and having values $k_0=8.12$, $k_\infty=3.72$, $C_1=2.47\times10^{11}$ N/m^3, $E_1=3.8$ eV, $T_D=837$ K, $m^*=0.318m_0$, and $K=0.21$ (current is perpendicular to c-axis).

As it can be seen in Fig. 3, measured temperature dependence of Hall mobility has a maximum value at the temperature about 220 K. Low temperature branch of the curve is strongly dependent on N_{dis} and N_A/N_D through μ_1 and μ_5 whereas the high temperature branch of carrier mobility is mainly defined by the polar optical phonon scattering mechanism, μ_4. Dislocation density, N_{dis}, is estimated using data obtained from cathodoluminescence (CL) measurements and estimated value for ZnO film is in the range of 6×10^8–3×10^9 cm^{-2}. Best fit to the experimental data is obtained for values of N_A/N_D in the range of 0.37–0.40. Such a relatively high value of N_A/N_D seems to be intrinsically related with the impurities and dislocations contained in the ZnO films. From the measurement of secondary ion mass spectroscopy (SIMS), some impurities such as the acceptors K, Na and the donors H, Al and Si are found in Fig. 4. The acceptors are rather largely incorporated than the donor impurities, which probably originated from the alumina tube for generating O_2 plasma. The fraction of activated species of both donors and acceptors cannot exactly calculated, however, large amounts of acceptor would be considered to have a contribution to increase the ratio of N_A/N_B. Moreover, large density of dislocation is known to be formed when II–VI semiconductor ZnO or III–V GaN has been heteroepitaxially grown [23]. Dislocation was known to capture electron and played as an acceptor and reported as much as about 10^{10} cm^{-3} for the ZnO films showing the mobility below 100 cm^2/V s. In this experiment, density of dislocation is approximately 6×10^8–3×10^9 cm^{-3} for the Zn-2, thus it also contribute to increase the ratio of N_A/N_D. This assumption agrees well with the previous report that the high ratio of N_A/N_D found in the ZnO thin film grown on ZnO/MgO double buffer layers on sapphire was closely related to the density of edge dislocation [13].

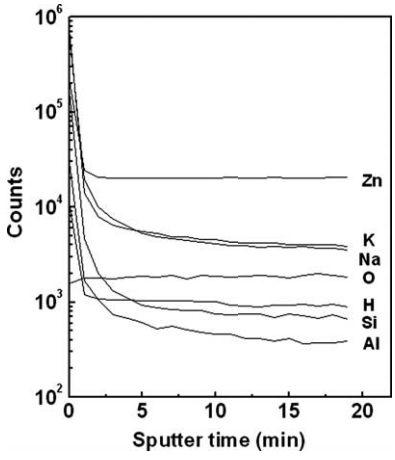

Fig. 4. SIMS depth profile for the ZN-2.

4. Conclusion

In summary, high quality ZnO films are grown on c-plane sapphire substrate using LT ZnO buffer layer by plasma-assisted molecular beam epitaxy. The film deposited at 720 °C shows the smallest value of FWHM for the symmetric (0002) diffraction peak of about 86 arcsec. The highest electron mobility in the films is about 103–105 cm^2/V s. The compensation ratio of acceptor concentration to donor one is about 0.37–0.40. From TDH measurements it can be supposed that hydrogen is source of n-type conductivity in the as-grown ZnO films.

Acknowledgements

This work was financially supported by the KIST Future-Resources Program Grant No. 2E18510 as well as the Korea Science and Education Foundation (KOSEF) Special Basic Research Program Grant No.R01-2004-000-10715-0. We gratefully acknowledge Dr G.N. Panin for cathodoluminescence measurements and valuable discussions.

References

[1] M. Kawasaki, A. Ohtomo, I. Ohkubo, H. Koinuma, Z.K. Tang, P. Yu, G.K.L. Wong, B.P. Zhang, Y. Segawa, Mater. Sci. Eng. B56 (1998) 239.
[2] D.C. Look, D.C. Reynolds, C.W. Litton, R.L. Jones, D.B. Eason, G. Cantwell, Appl. Phys. Lett. 81 (2002) 1830.
[3] K.K. Kim, H.S. Kim, D.K. Hwang, J.H. Lim, S.J. Park, Appl. Phys. Lett. 83 (2003) 63.
[4] Y.R. Ryu, T.S. Lee, H.W. White, Appl. Phys. Lett 83 (2003) 87.
[5] K. Vanheusden, W.L. Warren, C.H. Seager, D.R. Tallant, J.A. Voigt, B.E. Gnade, J. Appl. Phys. 79 (1996) 7983.
[6] D.C. Reynolds, D.C. Look, B. Jogai, H. Morco, Solid State Commun. 101 (1997) 643.
[7] D.C. Look, D.C. Reynolds, J.R. Sizelove, R.L. Jones, C.W. Litton, G. Cantwell, W.C. Harsch, Solid State Commun. 105 (1998) 399.
[8] D.C. Look, J.W. Hemsky, J.R. Sizelove, Phys. Rev. Lett. 82 (1999) 2552.
[9] D.C. Look, R.L. Jones, J.R. Sizelove, N.Y. Garces, N.C. Giles, L.E. Halliburton, Phys. Status Solidi A 195 (2003) 171.
[10] T. Nakamura, Y. Yamada, T. Kusumori, H. Minoura, H. Muto, Thin Solid Films 411 (2001) 60.
[11] Y.F. Chen, S.K. Kong, H.J. Ko, V. Kirshner, H. Wenisch, T. Yao, K. Inaba, Y. Segawa, Appl. Phys. Lett. 78 (2001) 3352.
[12] K. Miyamoto, M. Sano, H. Kato, T. Yao, J. Cryst. Growth 265 (2004) 34.
[13] K. Miyamoto, M. Sano, H. Kato, T. Yao, Jpn. J. Appl. Phys. 41 (2002) L1203–L1205.
[14] Y.S. Jung, Y.S. No, J.S. Kim, W.K. Choi, J. Cryst. Growth 267 (2004) 85.
[15] Y.S. Jung, O.V. Kononenko, J.S. Kim, W.K. Choi, J. Cryst. Growth 274 (2005) 418.
[16] C.G. Van de Walle, Physica B 308–310 (2001) 899.
[17] C.G. Van de Walle, Phys. Status Solidi B 229 (2002) 221.
[18] D.M. Hoffman, A. Hofstaetter, F. Leiter, H. Zhou, F. Henecker, B.K. Meyer, S.B. Orlinskii, J. Schmidt, P.G. Baranov, Phys. Rev. Lett. 88 (2002) 5504.
[19] K. Ip, M.E. Overberg, Y.W. Heo, D.P. Norton, S.J. Pearton, C.E. Stutz, B. Luo, F. Ren, D.C. Look, J.M. Zavada, Appl. Phys. Lett. 82 (2003) 385.
[20] Y.M. Strzhemechny, J. Nemergut, P.E. Smith, J. Bae, D.C. Look, L.J. Brillson, J. Appl. Phys. 94 (2003) 4256.
[21] B.K. Meyer, H. Alves, D.M. Hofmann, W. Kriegseis, D. Forster, F. Bertram, J. Christen, A. Hoffman, M. Strasburg, M. Dworzak, U. Haboeck, A.V. Rodina, Phys. Status Solidi B 241 (2004) 231.
[22] D.L. Rode, Semicond. Semimet. 10 (1975) 1.
[23] D.C. Look, Semicon. Sci. Technol. 20 (2005) S55.